

Protocols for Isolating and Characterizing Polysaccharides From 1 Plant Cell Walls: A Case Study Using Rhamnogalacturonan-II

Breeanna Urbanowicz (✉ breeanna@uga.edu)

University of Georgia <https://orcid.org/0000-0001-5247-4513>

William Barnes

University of Georgia Franklin College of Arts and Sciences

Sabina Koj

University of Georgia Franklin College of Arts and Sciences

Ian Black

University of Georgia Franklin College of Arts and Sciences

Stephanie Archer-Hartmann

University of Georgia Franklin College of Arts and Sciences

Parastoo Azadi

University of Georgia Franklin College of Arts and Sciences

Maria Pena

University of Georgia Franklin College of Arts and Sciences

Malcolm O'Neill

University of Georgia Franklin College of Arts and Sciences

Research Article

Keywords: Rhamnogalacturonan-II, Plant cell wall, Glycosyl residue, acetylation, methylation, Borate diester, Size-exclusion chromatography, Mass spectrometry, Nuclear magnetic resonance spectroscopy

Posted Date: February 12th, 2021

DOI: <https://doi.org/10.21203/rs.3.rs-216748/v1>

License: © ⓘ This work is licensed under a Creative Commons Attribution 4.0 International License.

[Read Full License](#)

Abstract

Background: In plants, there is a large diversity of polysaccharides that comprise the cell wall. Each major type of plant cell wall polysaccharide, including cellulose, hemicellulose, and pectin, has distinct structures and functions that contribute to wall mechanics and influence plant morphogenesis. In recent years, pectin modification and valorization has attracted much attention due to its expanding roles of pectin in biomass deconstruction, food science, material science, and environmental remediation. However, pectin utilization has been limited by our incomplete knowledge of pectin structure. Herein, we present a workflow of principles relevant for the characterization of polysaccharide primary structure using nature's most complex polysaccharide, rhamnogalacturonan-II (RG-II), as a model.

Results: We outline how to isolate RG-II from celery and duckweed cell wall material and red wine using chemical or enzymatic treatments coupled with size-exclusion chromatography. From there, we demonstrate the use of mass spectrometry (MS)-based techniques to determine the glycosyl residue and linkage compositions of the intact RG II molecule and RG-II-derived oligosaccharides including special considerations for labile monosaccharides. In doing so, we demonstrated that in the duckweed *Wolffiella repanda* the arabinopyranosyl (Arap) residue of side chain B is substituted at O-2 with rhamnose. As RG-II is further modified by non-glycosyl modifications including methyl-ethers, methyl-esters, and acetyl-esters, we then describe ways to use electrospray-MS to identify these moieties on RG-II-derived oligosaccharides. We then explored the utility of proton nuclear magnetic resonance spectroscopy (¹H-NMR) in identifying RG-II-specific sugars and non-glycosyl modifications to complement and extend MS-based approaches. Finally, we describe how to assess the factors that affect RG-35 II dimerization using liquid chromatographic and NMR spectroscopic approaches.

Conclusions: The complexity of pectic polysaccharide structures has hampered efforts aimed at their valorization. In this work, we used RG-II as a model to demonstrate the steps necessary to isolate and characterize polysaccharides using chromatographic, MS, and NMR techniques. The principles can be applied to the characterization of other saccharide structures and will help inform researchers on how saccharide structure relates to functional properties in the future.

Full Text

This preprint is available for [download as a PDF](#).

Figures

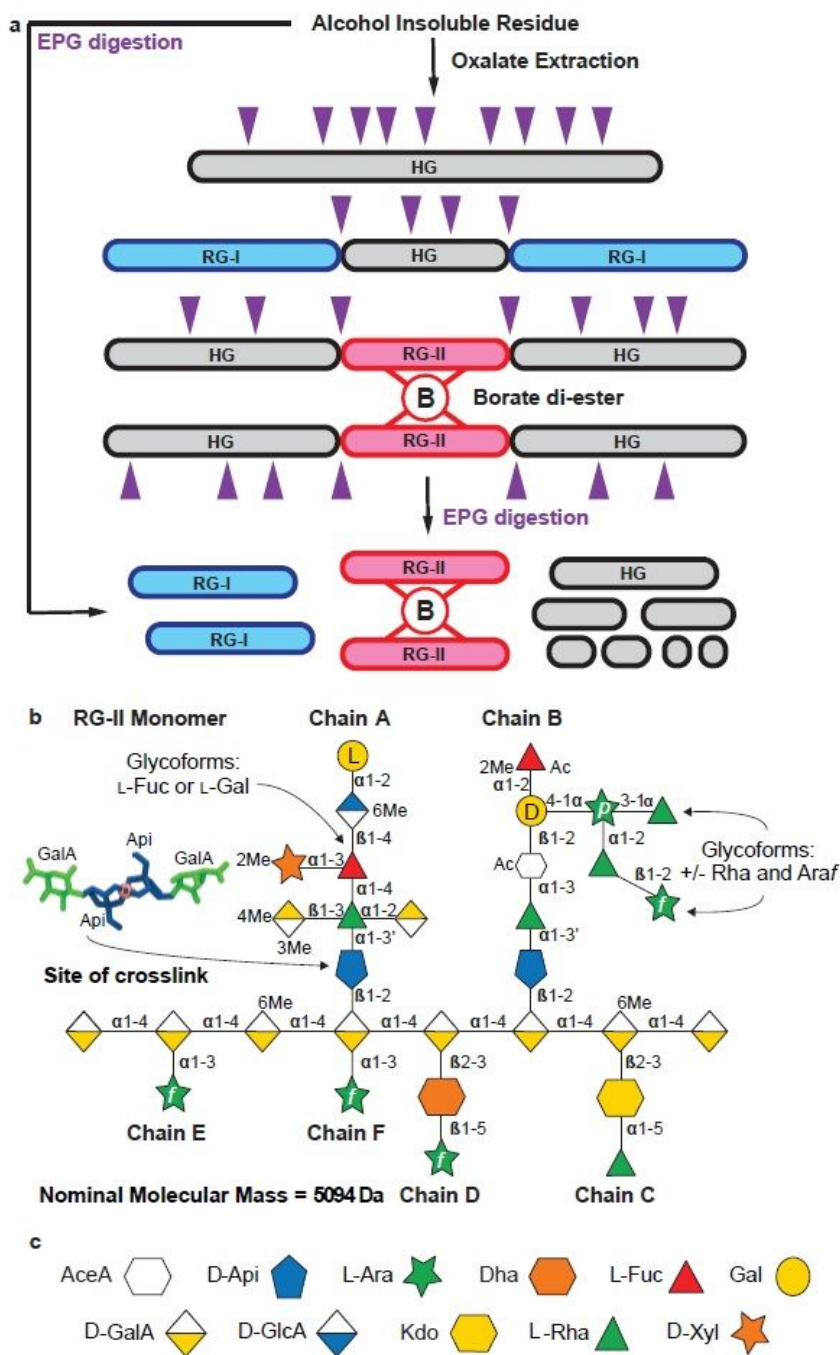


Figure 1

The isolation and glycosyl sequence of rhamnogalacturonan II. a. Schematic representation of the extraction of non-proteinaceous pectic domains including homogalacturonan (HG), rhamnogalacturonan-I (RG-I), and rhamnogalacturonan-II (RG-II) from alcohol insoluble residue (AIR) [22]. Covalently-linked multi-domain pectin molecules can be released by oxalate extraction if necessary (duckweed preparation). AIR or isolated multi-domain pectin molecules are then treated with endopolygalacturonase

(EPG) to hydrolyze the HG backbone to separate the pectic domains. Purple arrowheads represent sites of EPG cleavage on the HG backbone. b. The glycosyl sequence of the rhamnogalacturonan II (RG-II) monomer. The apiosyl residue involved in the formation of the borate diester cross linked dimer is shown. Also shown are the sites of structural diversity in RG-II glycoforms isolated from different plants with or without Araf and Rha extensions of side chain B and L-Fuc instead of L-Gal in side chain A. The RG-II structure depicted, which includes all of the known non-carbohydrate substituents, has a nominal molecular mass of 5094 Da. c. The RG-II-relevant symbols from the symbol nomenclature for glycans (www.ncbi.nlm.nih.gov/glycans/snfg.html).

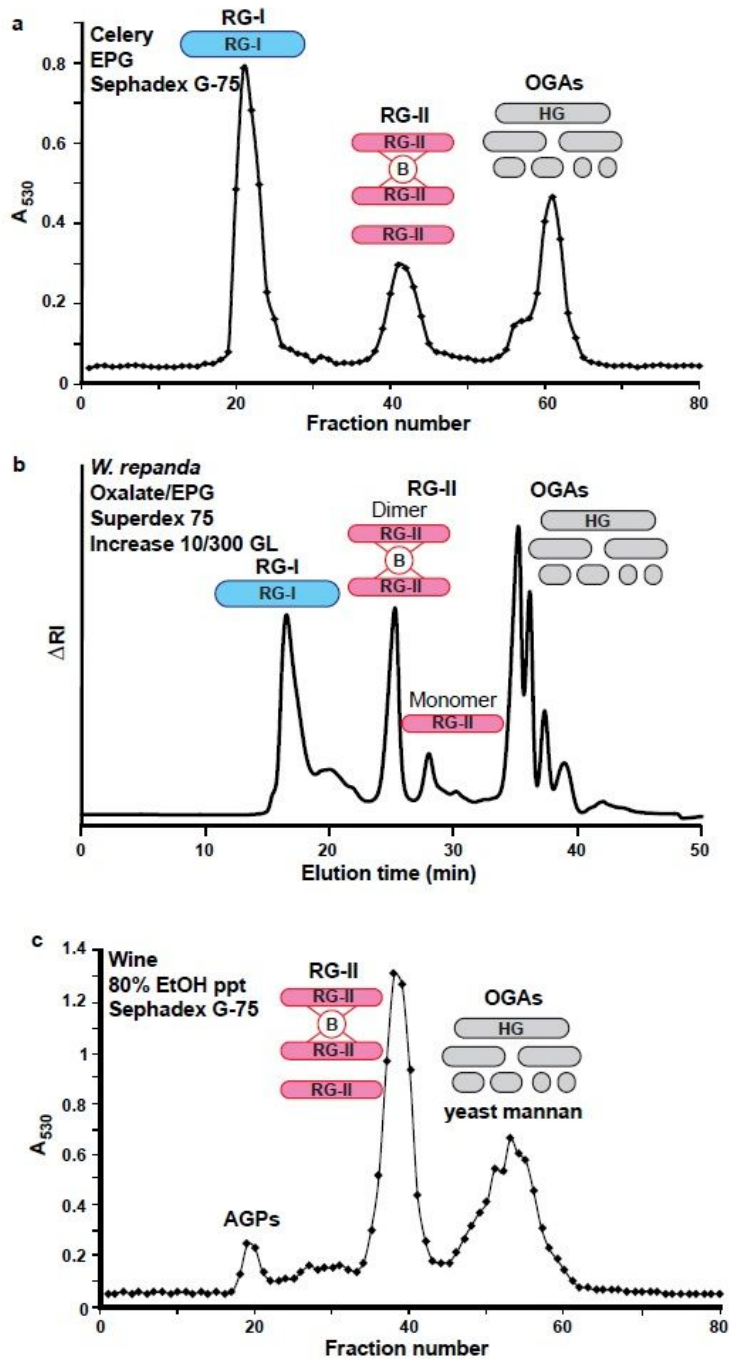


Figure 2

Isolation of RG-II using size-exclusion chromatography (SEC). a. EPG-solubilized material (200-300 mg) from celery AIR in 50 mM NaOAc pH 5 was fractionated using a preparative Sephadex G-75 SEC column (1 m x 4 cm). Fractions were assayed colorimetrically for uronic acids (A₅₃₀). b. SEC of the EPG-treated oxalate soluble fraction from *W. repanda* fractionated on a Superdex-75 Increase column monitored using refractive index (RI) detection. c. The ethanol precipitated material from red wine (~500 mg)

separated using a preparative Sephadex G-75 SEC column (1 m x 4 cm) and assayed colorimetrically for uronic acids (A530).

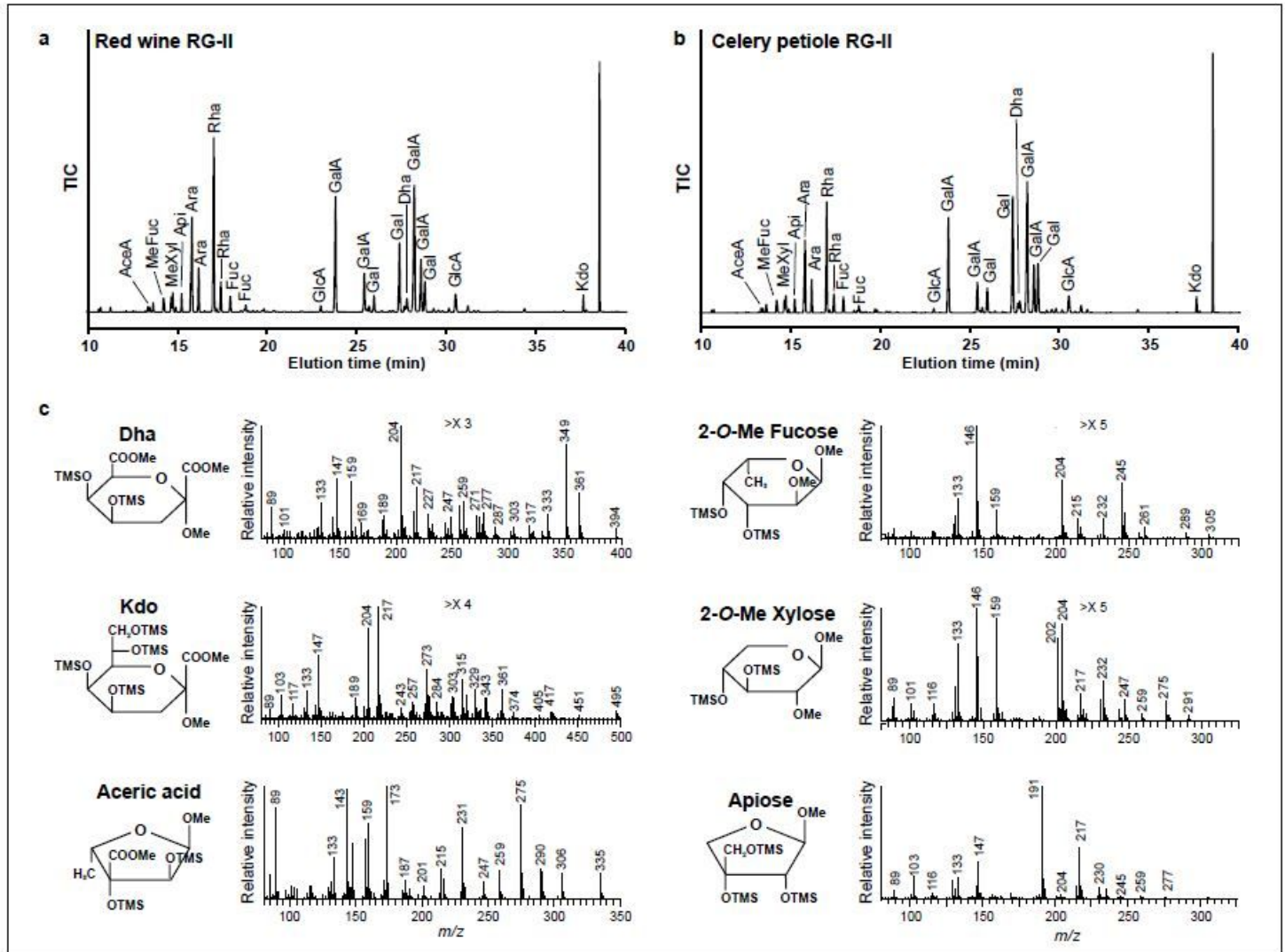


Figure 3

GLC-EI-MS total ion current profiles and selected mass spectra of the trimethylsilyl methyl glycoside derivatives of the monosaccharides generated from RG-II. a & b. The GLC EI-MS total ion current (TIC) profile of the TMS derivatives generated from wine (a) and celery (b) RG-II. The identity of the monosaccharide derivative in each peak is shown. The peak eluting at ~39 min is the TMS derivative of myo-inositol used as an internal standard. c. The EI mass spectrum of selected monosaccharide derivatives generated from wine RG-II. The multiplication factor (>X) used to expand selected regions of each mass spectrum is shown.

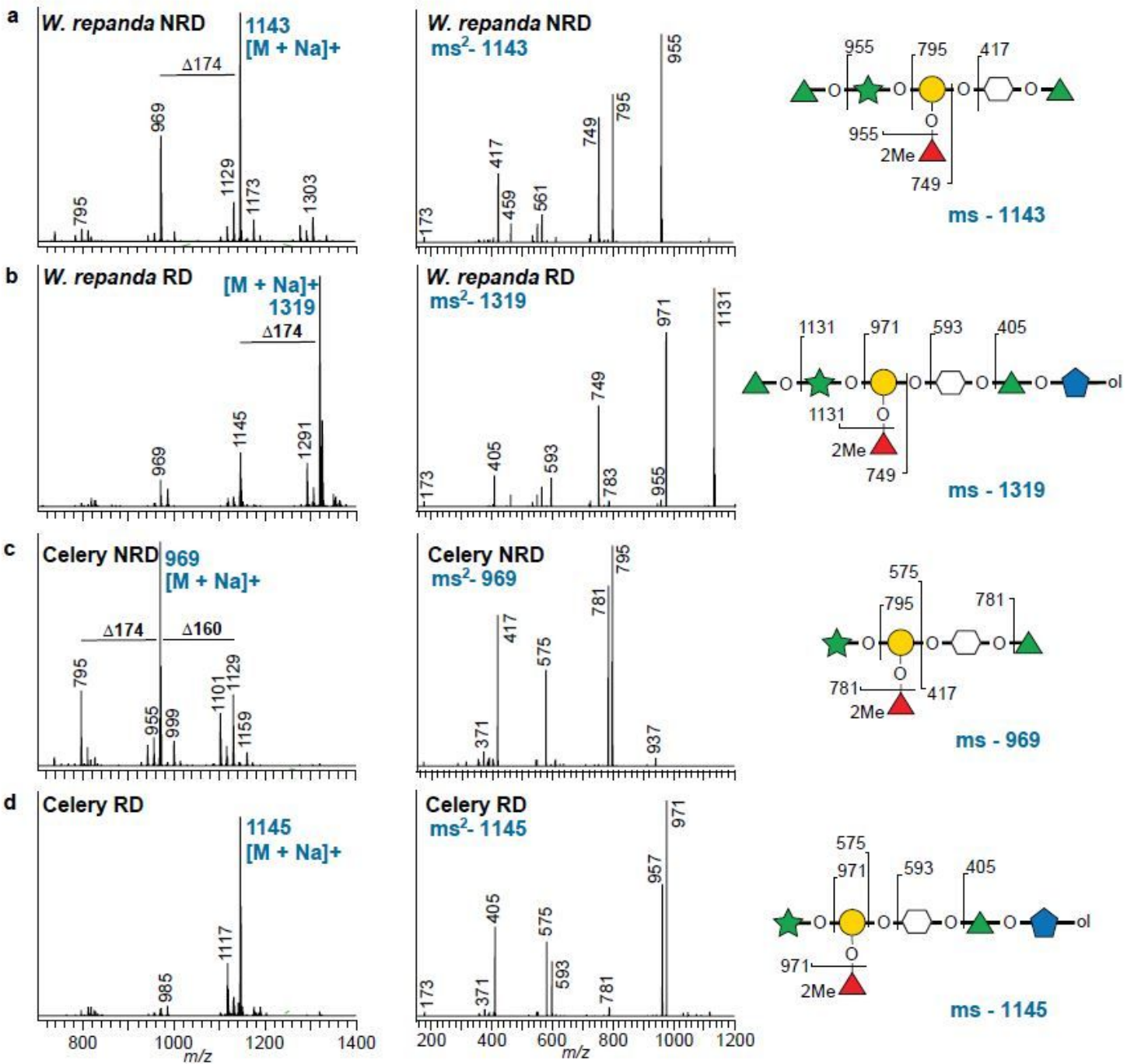


Figure 4

ESI-MS of side chain B released from RG-II by selective acid hydrolysis is degraded during methylation with solid NaOH and methyl iodide in DMSO. a. Methylated reducing B side chain oligosaccharides generated from *W. repanda* RG-II (left panel). The ms² spectrum (middle panel) and fragmentation pattern of the major ion (m/z 1143; right panel) is also shown. b. NaBH₄-reduced and methylated B side chain oligosaccharides generated from *W. repanda* RG-II (left panel). The ms² spectrum (middle panel) and fragmentation pattern of the major ion (m/z 1319; right panel) is also shown. c. Methylated reducing B side chain oligosaccharides generated from celery RG-II (left panel). The ms² spectrum (middle panel) and fragmentation pattern of the major ion (m/z 969; right panel) is also shown. d. NaBH₄-reduced and

methylated B side chain oligosaccharides generated from celery 1100 RG-II (left panel). The ms^2 spectrum (middle panel) and fragmentation pattern of the major ion (m/z 1145; right panel) is also shown. Refer to Fig. 1c for the relevant symbol nomenclature for glycans.

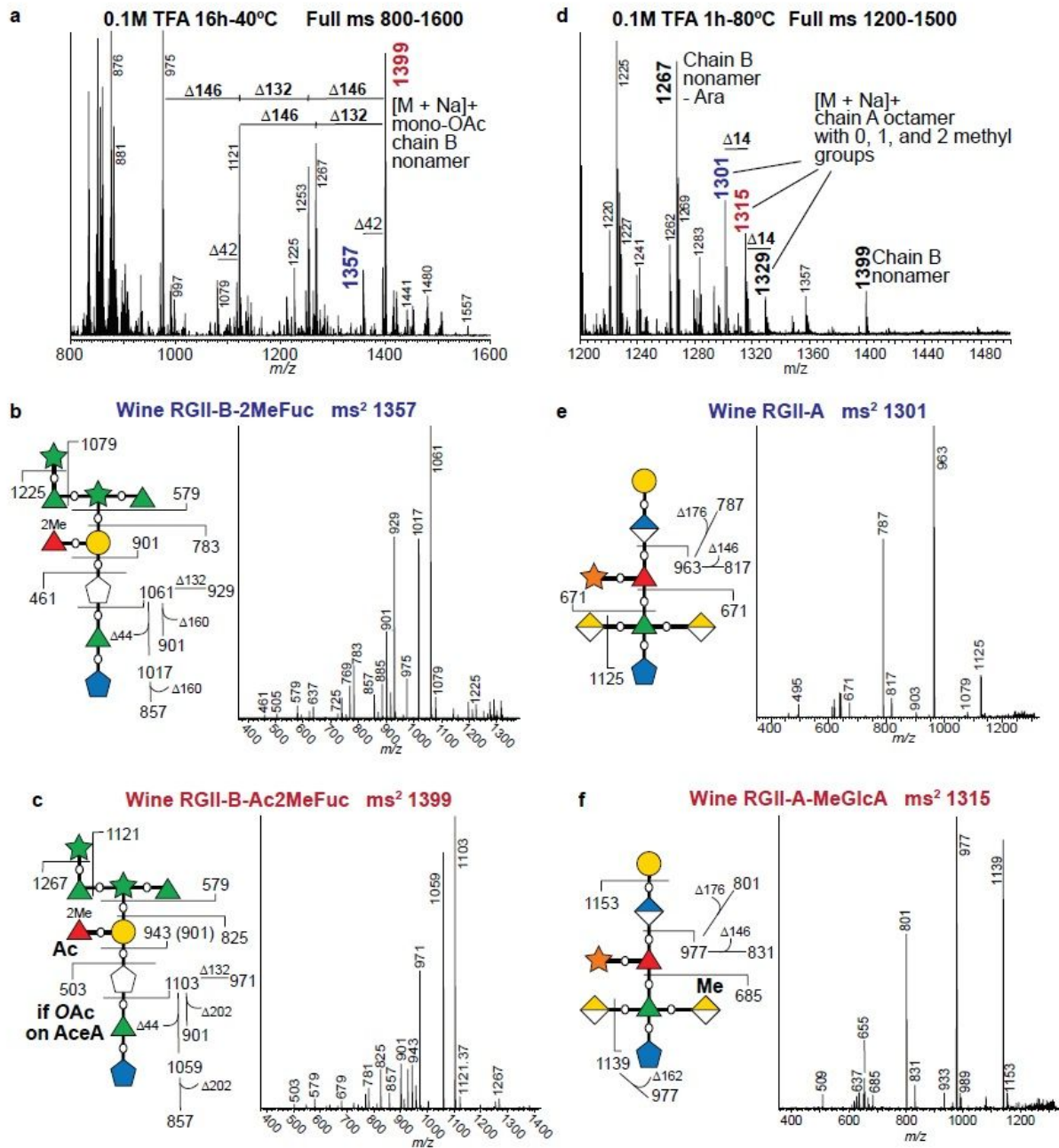


Figure 5

Locating the O-acetyl groups of side chain B and the methyl-ethers of side chain A using ESI-MS. a. The ESI mass spectrum of the oligosaccharides generated by treating wine RG-II with 0.1 M TFA for 16 h at 40°C (side chain B-enriched). $\Delta 146$ corresponds to a Rha residue, $\Delta 132$ corresponds to an Ara residue,

and $\Delta 42$ corresponds to an OAc group. b. The ms2 spectra of the B side chain nonasaccharide (m/z 1357) and its fragmentation pattern. c. The ms2 spectra of the B side chain mono-O-acetylated nonasaccharide (m/z 1399) and its fragmentation pattern. d. The ESI mass spectrum of the oligosaccharides generated by treating wine RG-II with 0.1 M TFA for 1 h at $80^\circ 1147$ C (side chain A-enriched). $\Delta 14$ corresponds to a methyl group. e. The ms2 spectra of the A side chain octasaccharide (m/z 1301) and its fragmentation pattern. f. The ms2 spectra of the A side chain mono-methylated octasaccharide (m/z 1315) and its fragmentation pattern. Refer to Fig. 1c for the relevant symbol nomenclature for glycans.

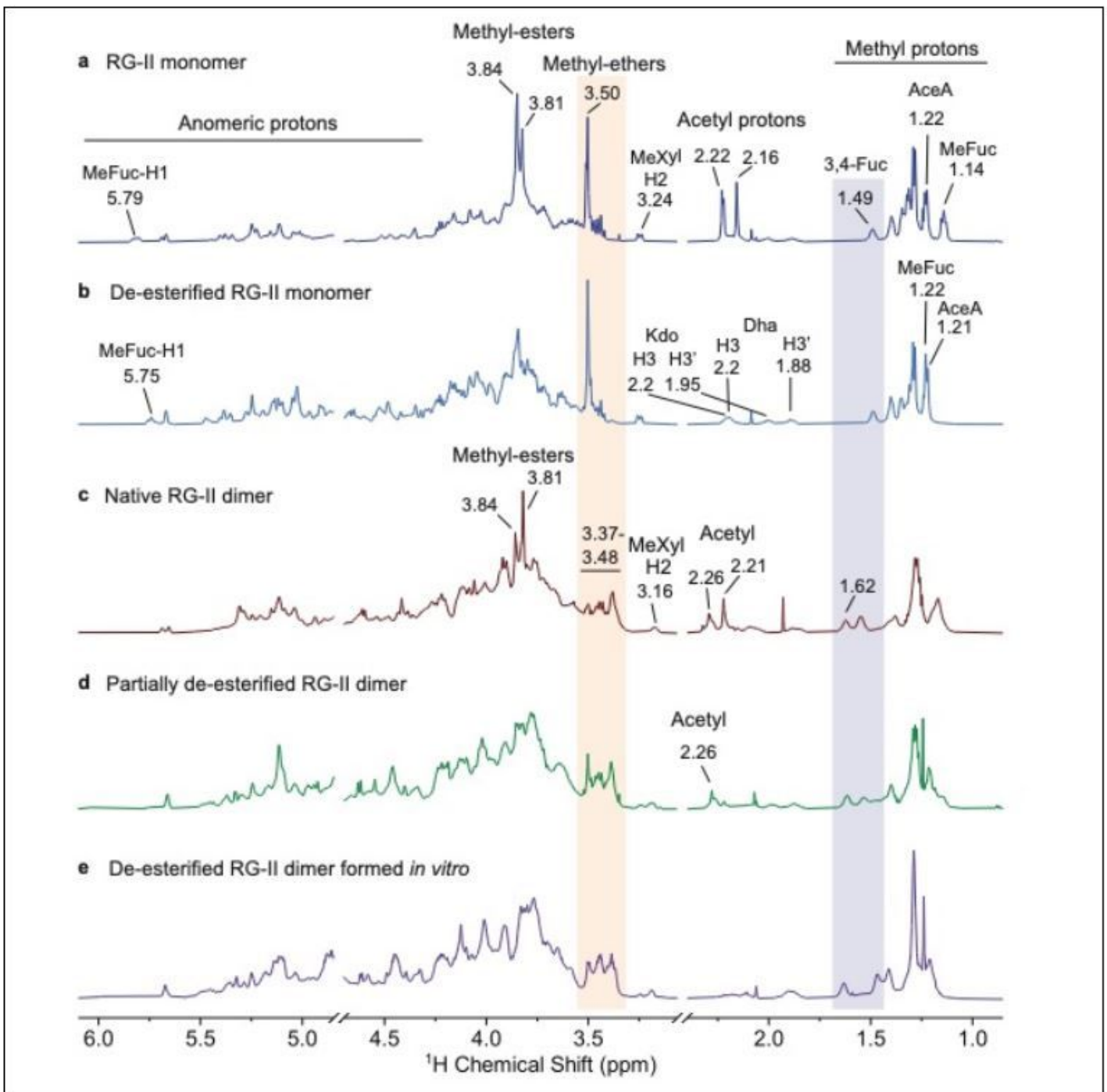


Figure 6

¹H NMR analysis of wine RG-II and the in vitro formed dimer. a. Wine RG-II monomer. b. De esterified RG-II monomer. c. Native RG-II dimer. d. Partially de-esterified RG-II dimer. e. RG-II dimer formed from the de-esterified RG-II monomer in vitro. The 1D ¹H NMR spectrum of the RG-II monomer (a) contains signals that correspond to acetyl and methyl groups. After base treatment, the signals of acetyl and methyl-esters are not observed in the spectrum of the de-esterified monomer (b), whilst the signals for methyl-ether remain. The removal of acetyl peaks revealed the presence of the diagnostic resonances of Kdo and Dha. The base treatment of the native dimer (c) removes methyl-esters but only partially de-acetylated the dimer (d). During in vitro dimerization of de-esterified monomer (e) several signals change. The more distinctive are the diagnostic resonances of methyl-ether (shaded orange) and 3,4 Fuc (shaded in blue), which have chemical shifts comparable to their counterparts in native and partially de-acetylated RG-II dimer.

Supplementary Files

This is a list of supplementary files associated with this preprint. Click to download.

- [Barnesetal.BfBAdditionalFile1.pdf](#)